Pergamon

Bioorganic & Medicinal Chemistry, Vol. 4, No. 8, pp 1255–1269, 1996

PII: S0968-0896(96)00122-8
0968-0896/96 $15.00+0.00

Molecular Structure and Dynamics of Some Potent 5-HT_3 Receptor Antagonists. Insight into the Interaction with the Receptor

Andrea Cappelli[a,*] Alessandro Donati,[b] Maurizio Anzini,[a] Salvatore Vomero,[a] Pier G. De Benedetti,[c] Maria Cristina Menziani[c] and Thierry Langer[d]

[a]*Dipartimento Farmaco Chimico Tecnologico, Università di Siena, Via Banchi di Sotto 55, 53100 Siena, Italy*
[b]*Dipartimento di Chimica, Università di Siena, Pian dei Mantellini, 53100 Siena, Italy*
[c]*Università degli Studi di Modena, Via Campi 183, 41100 Modena, Italy*
[d]*Institute of Pharmaceutical Chemistry, University of Innsbruck, Innrain 52A, A-6020 Innsbruck, Austria*

Abstract—The molecular structure and the dynamic behaviour of some potent 5-HT_3 antagonists structurally related to quipazine have been investigated by NMR spectroscopy and by computational methods in order to gain insight into the structure–activity relationships at a molecular level. The role of the different dynamic behaviour of these compounds in the binding to 5-HT_3 receptors is discussed. A model of ligand–receptor interaction has been developed on the basis of molecular orbital calculations and on the reference ligands quipazine, ondansetron and LY278584. The interaction model proposed herein rationalizes the observed agonist–antagonist shift between quipazine and investigated compounds with the assumption of different but overlapping binding domains for antagonists and agonists at the 5-HT_3 receptor. Copyright © 1996 Elsevier Science Ltd

Introduction

Serotonin exerts its actions through several (5-HT) receptors which are classified into at least four main types (5-HT_1, 5-HT_2, 5-HT_3, 5-HT_4). The 5-HT_3 antagonists represent pharmacologically interesting compounds in the treatment of emesis induced by antitumoral therapy; their potential uses in several other disorders (migraine, generalized anxiety, schizophrenia, drug addiction, age related memory impairment, etc.) have been intensively investigated.[1] Quipazine is an arylpiperazine which has attracted only little interest on the part of medicinal chemists, despite its high affinity for 5-HT_3 receptors. This piperazinyl quinoline was reported to behave as a 5-HT_3 antagonist in peripheral models,[2] but 5-HT_3 receptor binding studies with rat cortex membrane gave a Hill number higher than unity, raising the question whether quipazine displays agonist activity at central 5-HT_3 receptors.[3] An initial answer was recently provided by Emerit and coworkers who described quipazine as a 5-HT_3 receptor agonist in the '[^{14}C]guanidinium accumulation test' applied to NG 108–15 cells.[4] It is noteworthy that the 5-HT_3 receptor expressed by NG 108–15 cells is very similar to that present in the rat cortex.[5] We have very recently reported on the synthesis and pharmacological activity of a series of 5-HT_3 receptor ligands structurally related to quipazine.[6] Among these ligands, compounds **1–3** bound 5-HT_3 receptors labeled in rat cortical membrane by tritiated granisetron with high affinity and selectivity. Furthermore, these compounds behaved as 5-HT_3 receptor antagonists in the '[^{14}C]guanidinium accumulation test' in NG 108–15 cells. In that paper, we also discussed the structure–affinity relationships, and one of the features which mostly attracted our attention was the fact that compounds **1** and **4** differ significantly in their 5-HT_3 receptor affinity, although they show similar geometries.

In this study the molecular structure and dynamic behaviour of compounds **1**, **2** and **4** have been investigated by NMR spectroscopy and by computational methods in order to gain insight into the structure–activity relationships of this interesting class of 5-HT_3 receptor antagonists, at the molecular level. The role of the different dynamic behaviour of these compounds in the binding to 5-HT_3 receptors is discussed and a model of ligand–receptor interaction has been developed on the basis of molecular orbital calculations performed on compounds **1–4** and on the reference ligands ondansetron, LY278584,[7] and quipazine. The interaction model described herein accounts for the agonist–antagonist shift between quipazine and compounds **1–3** and implies different but overlapping binding domains for antagonists and agonists at the 5-HT_3 receptor.

Key words: Serotonin 5-HT_3 receptors; 5-HT_3 receptor antagonists; 5-HT_3 receptor mapping; molecular dynamics; molecular orbital calculations.

Results

NMR studies

Comparative information on the molecular structure and the dynamic behaviour of compounds **1**, **2** and **4** in

solution can be obtained by NMR studies. In this study we focused mainly on the condensed heterocyclic system, which modulates the affinities of this highly congeneric class of 5-HT_3 antagonists.

^{1}H NMR assignment

While the ^{1}H NMR spectrum of **2** was well resolved at 200 MHz, the ^{1}H NMR spectrum of **1** showed that the aromatic peaks overlap almost completely. Thus **1** and **2** were studied by high field (600 MHz) ^{1}H NMR spectroscopy with standard 1D and 2D (COSY and NOESY) techniques, and a complete ^{1}H assignment was achieved.

Figure 1 shows the aromatic regions of ^{1}H NMR spectra of **1** and **2** at 600 MHz. Owing to the high similarity between the structures of **1** and **2**, in the assignment of the ^{1}H NMR signals we assumed that quinoline signals of H-10 and H-9 (of compounds **1** and **2**, respectively) are located at nearly the same position.

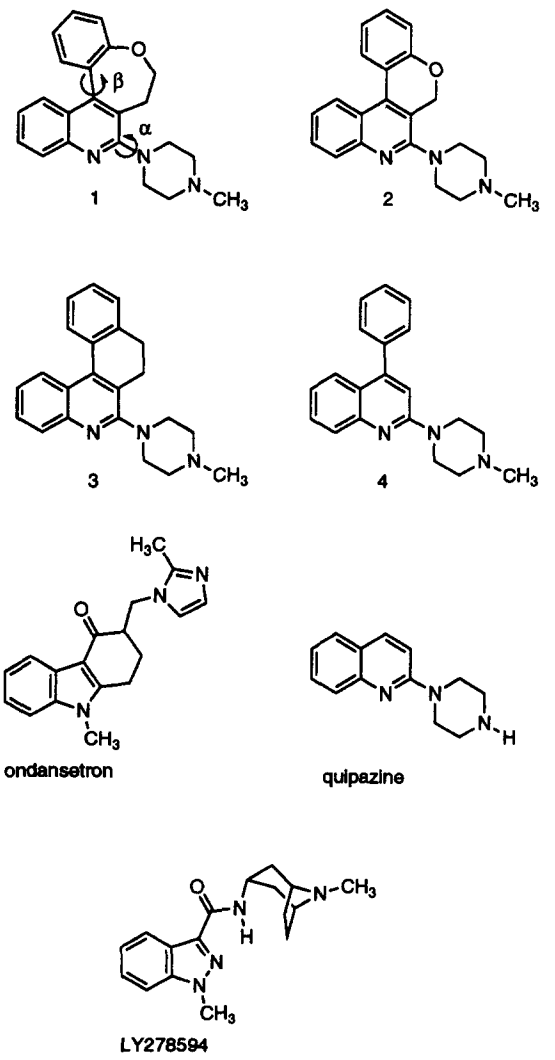

Chart 1.

Furthermore, H-4 of both compounds **1** and **2** should show the highest field doublets of the aromatic region. On this assumption, the ^{1}H NMR resonances of **2** were assigned by 2D-COSY and NOESY analysis.

The key information afforded by the NOESY spectrum of **2** is the cross-peak between the two lowest field doublets. This indicates a dipolar connection between two protons located in different parts of the molecule but relatively close to each other in space because of the conformation of the complex heterocyclic system. Thus, the signals at δ 8.37 and 8.02 were assigned to the H-12 and H-1 protons, respectively. The other scalar and dipolar connectivities confirmed the assumption and allowed a reliable assignment. A similar dipolar interaction was also observed in the NOESY spectrum of **1** between the doublets at δ 7.49 and 7.86. The intensity of the cross-peak was clearly lower than that of the corresponding one of **2**. This difference could be easily explained by considering the different geometry of **1** and **2**.

Table 1 summarises the complete assignment of ^{1}H NMR signals of compounds **1** and **2**.

The comparison of the (^{1}H NMR) aromatic regions of **1** and **2** (Fig. 1) shows the clear lower field shift of a well defined set of frequencies from **1** to **2**, corresponding to the protons located in the 'ansa' region of the condensed heterocyclic system. This appears to be consistent with a lower dihedral angle between the planes of the two aromatic rings of the molecules. Along with lower field shifts, higher field shifts were also observed for H-2, H-3 and H-4. This effect is probably due to a disfavoured oxygen lone-pair delocalization in compound **1** because of the higher seven-membered ring strain.

The assignment of compound **4** ^{1}H NMR signals was closely derived from the assignment of ^{1}H NMR signals of the upper homologous 2-(4-ethyl-1-piperazinyl)-4-phenylquinoline reported in the literature.[8]

Structure of 1 and 2 in solution

The aliphatic region of the 600 MHz ^{1}H NMR spectrum of compound **1** in $CDCl_3$ shows an ABMX spin system signal pattern with multiplets centred at 4.56 (unresolved AB peaks), 3.07 (M) and 2.75 (X), and attributable to the diastereotopic C-6 and C-7 methylene protons, respectively, a sharp singlet at δ 2.38, a broad singlet at δ 2.64 and an A_2B_2 multiplet centred at 3.35 due to N-CH_3 and 3′-5′ and 2′-6′ piperazine methylenes, respectively.

When the ^{1}H NMR spectrum was performed at 200 MHz, a similar signal pattern was found, with a difference concerning the methylene protons of piperazine which appeared as two triplets. By using benzene-d_6 instead of $CDCl_3$ as solvent at the same frequency, a good improvement in the resolution of the spectral lines of the ABMX spin systems was observed, and the signal attributable to 2′-6′ piperazine methylene

protons appeared as an A_2B_2 multiplet as in the 600 MHz spectrum. The appearance of C-6 and C-7 methylene protons as an ABMX spin system and of 2′-6′ piperazine methylene signals as an A_2B_2 system is compatible with the non-planar disymmetric arrangement of the condensed heterocyclic system showed by **1** in the crystal. Furthermore, the possible seven-membered ring inversion seems to be slow in 200 MHz ^{1}H NMR time scale. Thus, the determination of the coupling constants (J) of the ABMX spin system was attempted in order to obtain interesting information about the structure present in solution.

Thus, the determination of the coupling constant was attempted with the aid of homo-decoupling experiments. Unfortunately, these experiments failed to give reliable results.

A precise determination of the coupling constants in the ABMX spin-system was achieved by performing 2D J-resolved experiments at 600 MHz using benzene-d_6 as solvent.

Interestingly, such experimentally determined J values were very similar to the theoretically calculated ones (Macromodel)[9] for one of the three structures found in the asymmetric unity of **1** determined by X-ray diffraction studies.[6]

In Figure 2 the theoretical and the experimental ABMX spin-system J values of **1** are reported.

These findings strongly suggest that the structure in solution determined by ^{1}H NMR spectroscopy is very similar to that of the compound in the solid state. Furthermore, the condensed heterocyclic system of compound **1** appears to be very rigid.

In comparison, compound **2** shows a much simpler 200 MHz ^{1}H NMR aliphatic signal pattern in both $CDCl_3$ and benzene-d_6 as solvent: the piperazine methylene signals appear as two triplets at δ 2.66 and 3.35, respectively and the C-6 methylene signal is a sharp singlet.

This seems to suggest a higher degree of mobility of the condensed heterocyclic system of **2**.

Finally, in the ^{1}H NMR spectrum of compound **4** performed at 200 MHz, the piperazine methylene signals appeared as two triplets in both $CDCl_3$ and in benzene-d_6 as in the case of compound **2**. Interestingly, the signal attributable to the protons of the phenyl substituent appeared as a sharp singlet in $CDCl_3$, but was split into two multiplets when benzene-d_6 was used as solvent.

However, only very crude information about molecular dynamics could be obtained (e.g., a rough distinction

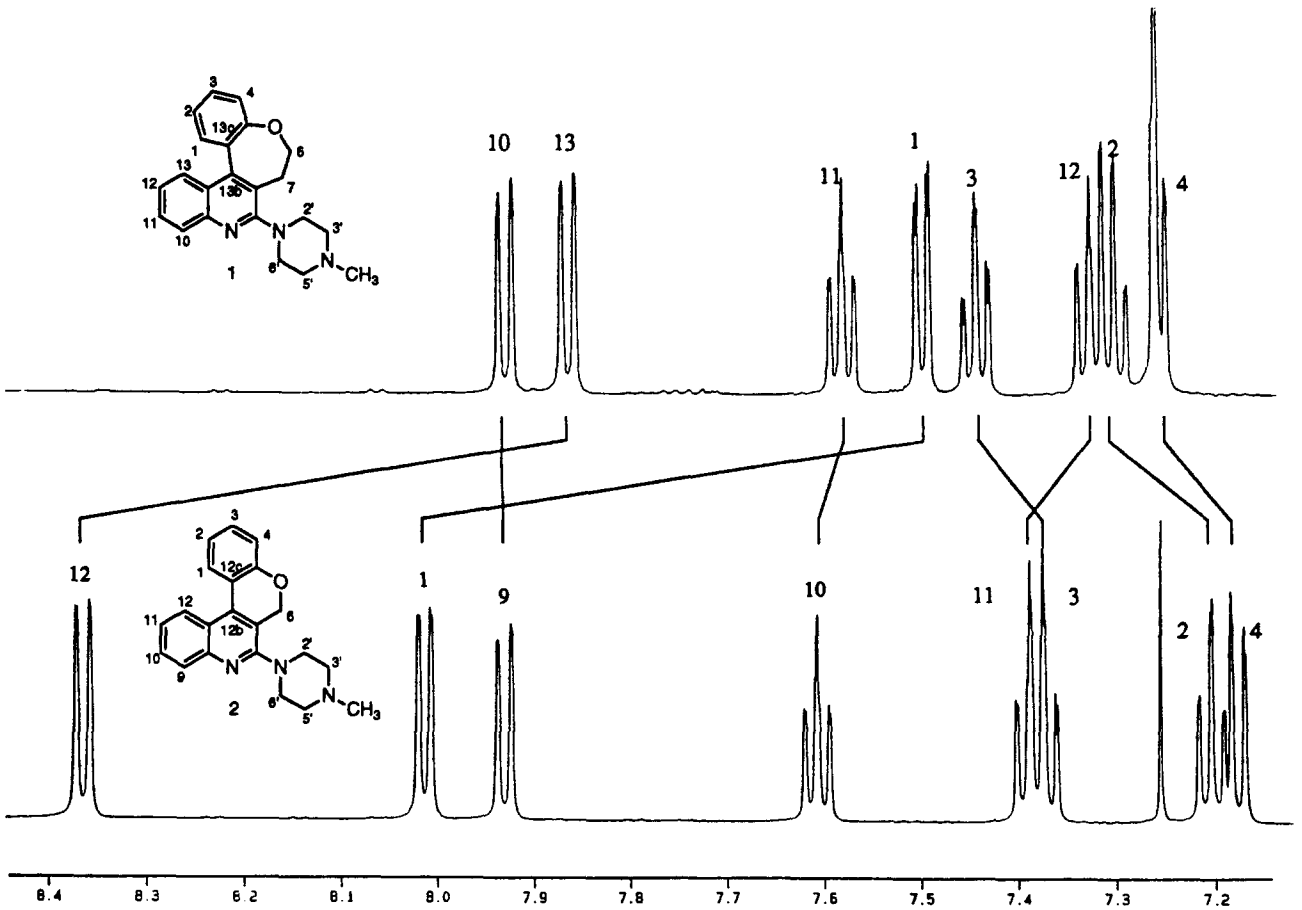

Figure 1. Superimposition of the ^{1}H NMR spectra of the aromatic regions of **1** and **2**.

between the rapid and the slow motions in the time scale of ^{1}H NMR) from the analysis of the standard ^{1}H NMR spectra.

^{13}C NMR relaxation rate studies

In order to obtain information about rapid motions, compounds **1**, **2** and **4** were studied by ^{13}C NMR relaxation rate analysis. This technique gives information about the molecular motions which occur in the ps time scale.[10]

Protonated ^{13}C NMR frequencies were assigned on the basis of 2D ^{1}H–^{13}C NMR HETCOR experiments performed at 600 and 200 MHz on **1** and **2** and **4**, respectively. Quaternary ^{13}C NMR frequencies were not assigned.

Table 1. ^{1}H NMR chemical shift of compounds **1** and **2** measured at 600 MHz[a]

1		2	
H	δ (ppm)	H	δ (ppm)
10	7.92	9	7.93
13	7.86	12	8.37
11	7.57	10	7.61
1	7.49	1	8.02
3	7.43	3	7.37
12	7.31	11	7.40
2	7.28	2	7.20
4	7.23	4	7.17
6	4.56	6	5.05
2′-6′	3.35	2′-6′	3.35
7	3.07	—	—
7	2.75	—	—
3′-5′	2.64	3′-5′	2.66
Me	2.38	Me	2.42

[a]The relative chemical shifts of **2** are not in decreasing order for better comparison with those of **1**.

Tables 2–4 show the ^{13}C NMR chemical shift (δ) values of **1**, **2** and **4**, respectively, along with the experimental ^{13}C NMR relaxation rates (R_1) and the calculated correlation time (τ_c).

Under the present experimental conditions we assumed a completely dipolar relaxation, and the correlation time which modulates the proton–carbon dipolar coupling was determined by eq (1).[11]

$$R_1 = \frac{1}{10}\frac{\hbar^2\gamma_H^2\gamma_C^2}{r_{C-H}^6}\left(\frac{3\tau_c}{1+\omega_C^2\tau_c^2}+\frac{6\tau_c}{1+(\omega_H+\omega_C)^2\tau_c^2}+\frac{\tau_c}{1+(\omega_H-\omega_C)^2\tau_c^2}\right) \quad (1)$$

At first sight it is rather difficult to find a relationship between the τ_c values and the possible motion of the condensed heterocyclic systems of compounds **1** and **2** because the τ_c values also change in the case of carbon atoms belonging to the same rigid moiety (e.g., quinoline nucleus or phenyl substituent). Moreover, it is difficult to determine the existence of preferred rotation axes of the entire molecules. However, it should be noted that in both compounds **1** and **2**, the τ_c average values for the carbon atoms of the quinoline nucleus were found to be greater than those for the phenyl substituent. While this difference in compound **2** is not significant, being about 2%, in compound **1** it becomes more relevant, being about 9%.

In absolute terms even a difference of 9% could be non-significant because there are some carbon atoms on the same rigid moiety which differ by 15–19% from the τ_c average value. However, since this difference is used for an internal comparison, it is in fact meaningful.

Based on the results of the ^{13}C NMR relaxation rate analysis, the condensed heterocyclic system of **1** is

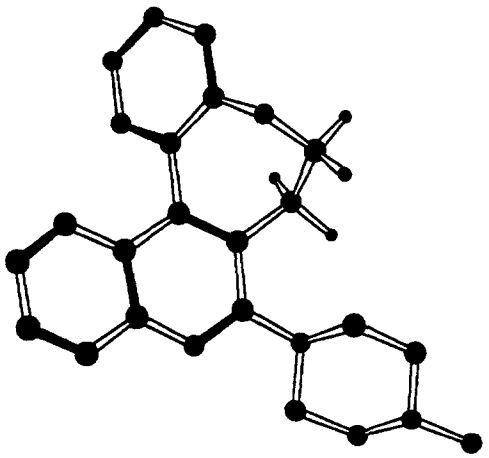

Spin System	J (Hz) Theoretical	Experimental	Dihedral Angle (degree)
AB	–	9.7	–
AM	4.3	4.0	-45.3
AX	11.6	12.6	-164.8
BM	0.5	1.0	73.5
BX	6.2	6.2	-45.2
MX	–	14.0	–

Figure 2. Coupling constants (J) in the ethyleneoxy bridge ABMX spin system of compound **1**. The theoretical J values were calculated within Macromodel on one of the three structures of the asymmetric unity of **1** found by X-ray diffraction studies.

Table 2. ^{13}C NMR chemical shift (δ), relaxation rate (R_1) and correlation time (τ_c) of compound **1** measured at 200 MHz

C	δ (ppm)	R_1[a] (s^{-1})	τ_c (s)
Q[b]	160.04	—	—
Q	155.21	—	—
Q	146.87	—	—
Q	144.90	—	—
1	131.38	1.241	5.50×10^{-11}
Q	131.25	—	—
3	129.93	1.427	6.33×10^{-11}
11	128.38	1.286	5.70×10^{-11}
10	128.31	1.396	6.19×10^{-11}
13	125.17	1.452	6.45×10^{-11}
12	124.33	1.503	6.67×10^{-11}
Q	123.77	—	—
2	123.71	1.356	6.01×10^{-11}
Q	123.57	—	—
4	122.53	1.120	4.96×10^{-11}
6	78.90	1.143	5.06×10^{-11}
3′-5′	55.10	0.977	4.32×10^{-11}
2′-6′	50.87	0.981	4.34×10^{-11}
Me	46.10	0.545	2.40×10^{-11}
7	27.66	1.278	5.67×10^{-11}

[a]The reported relaxation rates of the protonated carbons are referred to a single ^{1}H–^{13}C relaxation vector.
[b]Quaternary carbon.

likely to be more flexible than that of **2**. Thus, these results seem to contradict the dynamic picture obtained through the analysis of the standard ^{1}H NMR spectra.

A rationalization of the overall results can be found by splitting the global dynamic behaviour of **1** and **2** into a component of slow motions and one of rapid motions.

Table 3. ^{13}C NMR chemical shift (δ), relaxation rate (R_1) and correlation time (τ_c) of **2** measured at 200 MHz

C	δ (ppm)	R_1[a] (s^{-1})	τ_c (s)
Q[b]	157.45	—	—
Q	156.90	—	—
Q	147.99	—	—
Q	136.66	—	—
3	130.14	1.181	5.23×10^{-11}
9	128.89	1.041	4.61×10^{-11}
10	128.86	1.000	4.42×10^{-11}
1	128.28	1.009	4.46×10^{-11}
12	124.68	1.126	4.99×10^{-11}
11	124.53	1.200	5.32×10^{-11}
Q	123.03	—	—
2	121.97	1.227	5.44×10^{-11}
Q	121.31	—	—
Q	121.08	—	—
4	117.58	0.866	3.83×10^{-11}
6	65.37	1.176	5.21×10^{-11}
3′-5′	55.12	0.872	3.85×10^{-11}
2′-6′	49.86	0.933	4.13×10^{-11}
Me	46.20	0.586	2.59×10^{-11}

[a]The reported relaxation rates of the protonated carbons are referred to a single ^{1}H–^{13}C relaxation vector.
[b]Quaternary carbon.

Table 4. ^{13}C NMR chemical shift (δ), relaxation rate (R_1) and correlation time (τ_c) of **4** measured at 200 MHz

C	δ (ppm)	R_1[a] (s^{-1})	τ_c (s)
Q[b]	157.70	—	—
Q	150.26	—	—
Q	149.83	—	—
Q	140.13	—	—
2″-6″-7[c]	130.10	0.491	2.05×10^{-11}
3″-5″	128.96	0.413	1.72×10^{-11}
4″	128.51	0.725	3.03×10^{-11}
8[d]	128.30	0.470	1.96×10^{-11}
5	126.27	0.852	3.56×10^{-11}
Q	123.02	—	—
6	122.98	0.938	3.92×10^{-11}
3	110.50	0.774	3.23×10^{-11}
3′-5′	55.59	0.559	2.33×10^{-11}
Me	46.58	0.349	1.46×10^{-11}
2′-6′	45.68	0.517	2.16×10^{-11}

[a]The reported relaxation rates of the protonated carbons are referred to a single ^{1}H–^{13}C relaxation vector.
[b]Quaternary carbon.
[c]Assuming for C-2″ and C-6″ the same τ_c value found for C-3″ and C-5″ (17.2 ps) and for C-7 the same value found for C-6 (39.2 ps), the calculated mean, 24.5 ps, appears to be very similar to that actually found for the signal at δ 130.10.
[d]Because of the proximity of this signal with one of the benzene-d_6 peaks, its T_1 value (and consequently its τ_c value) is not to be considered thoroughly reliable.

The phenyl substituent of **2** has probably negligible rapid motions, and the inversion of the pyrano ring occurs with a low frequency (slow motion component), but is high enough to mediate the signal of the pyrano methylene protons (high frequency of the inversion in the time scale of ^{1}H NMR at 200 MHz).

On the contrary, compound **1** possesses two components of the motion: a component of rapid vibrations of the phenyl substituent within a narrow angle around the position of the energy minimum (dihedral angle about 50°) and a slow component of inversion of the seven-membered ring.

This reorientation process occurs with low frequency in the time scale of ^{1}H NMR at 200 MHz and the oxepine methylene proton signals are not mediated.

In both compounds **1** and **2** the τ_c average values of the carbon atoms of the piperazine moiety are significantly lower than the respective values of the carbon atoms of the quinoline nucleus suggesting the presence of a local mobility in the piperazine moiety of these two compounds.

When this kind of analysis was applied to the τ_c values of the carbon atoms of **4** a higher mobility of the phenyl substituent of this compound was found. In fact, the τ_c average values of the carbon atoms of the quinoline nucleus differ from those of the phenyl substituent by about 40%, while the mobility of the piperazine

moiety seems to be similar to that of the same moiety of **1** and **2**.

It is noteworthy that these speculations acquire a particular importance if the models of the dynamic behaviour of compounds **1**, **2** and **4** obtained from the experimental NMR studies are compared with those obtained from the computational theoretical approach, as an overall agreement is found.

Variable temperature ^{1}H NMR studies on compound 1

In order to obtain further information about the component of the slow molecular motions present in the condensed heterocyclic system of **1**, this compound was studied by ^{1}H NMR experiments performed at different temperatures.

As previously reported, the oxepine methylene signals appear as an ABMX spin-system in the aliphatic region of the ^{1}H NMR spectrum of **1** in $CDCl_3$ at 200 MHz. This indicates that the hindrance to internal reorientation along the C-13b/C-13c (Fig. 1) bond must be rather high, making the rate of exchange between the two atropoisomeric conformations too slow at room temperature to average out the resonance shift between the methylene protons.

In order to calculate the reorientation barrier, ^{1}H NMR spectra at variable temperature were performed at 200 MHz in nitrobenzene-d_5. During the NMR measurements at variable temperature, coalescence of the C-7 methylene (X and M) was observed (Fig. 3), and the coalescence temperature of 410 K was chosen to calculate the reorientation barrier following the method of Gutowsky and Holm (GH-method).[12]

In Table 5, the experimentally observed signal separation at the various temperatures ($\delta\omega_e$) and the values of $1/\tau\delta\omega$ calculated using the GH-method are reported. Equation 2 was used in the calculation of the $1/\tau\delta\omega$ value.[13]

$$\frac{1}{\tau\delta\omega}=\sqrt{\frac{1}{2}-\frac{1}{2}\left(\frac{\delta\omega_e}{\delta\omega_\infty}\right)^2} \qquad (2)$$

The data in Table 5 are plotted in Figure 4 as $\ln(1/\tau\delta\omega)$ vs. $1000/T$, giving points which are fitted reasonably well by (3). The data are reported in Table 6.

$$\ln\frac{1}{\tau\delta\omega}=\ln\frac{2\nu_0}{\delta\omega}-\frac{E_a}{RT} \qquad (3)$$

By using the Eyring absolute reaction rate equation,[14] a ΔG^* value of 21.3 kcal/mol at T_c 137 °C (410 K) was calculated from Arrhenius parameters E_a[15] and ν_0. Furthermore, from the Arrhenius expression $k=3.36\times10^6\exp(-9.25/RT)$, given $k=1/2\tau$ the half-life (τ) of the atropoisomeric forms of **1** at room temperature and the optical stability could be extrapolated.

A value of $\tau=0.9$ s is compatible with the structure of the oxepine methylene proton signals (ABMX spin system), and accounts for the failure in the resolution of **1** (vide infra in Chemistry section).

Finally, in the time scale of the interaction with the receptor (we calculated a $t_{1/2}$ of about 3 min for the interaction of **1** with 5-HT_3 receptors),[16] the reorientation of the condensed heterocyclic system of **1** appears to be very slow motion.

Computational studies

Molecular dynamics. Molecular dynamics simulations were performed on compounds **1**, **2** and **4**. The analysis

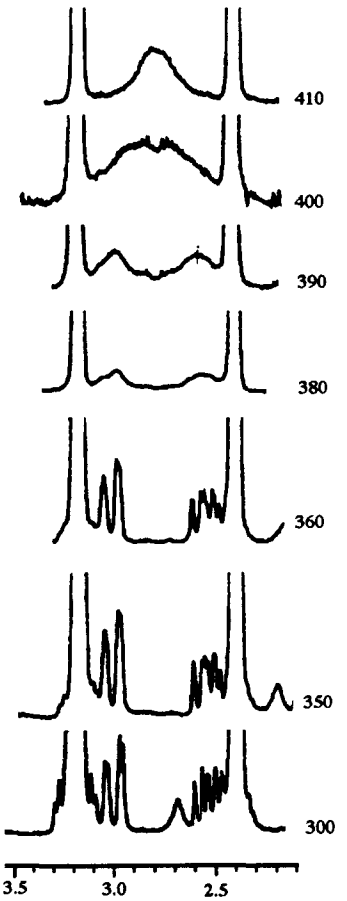

Figure 3. Temperature dependence of ^{1}H NMR signals of the C-7 methylene protons of **1**.

Table 5. Temperature dependence of the experimental $\delta\omega_e$ and $1/\tau\delta\omega$

Temperature (K)	$\delta\omega_e$ (Hz)	$1/\tau\delta\omega$
300	97.8	0.000
350	96.5	0.115
360	94.8	0.174
380	87.7	0.313
390	80.2	0.405
400	30.1	0.673
410	—	—

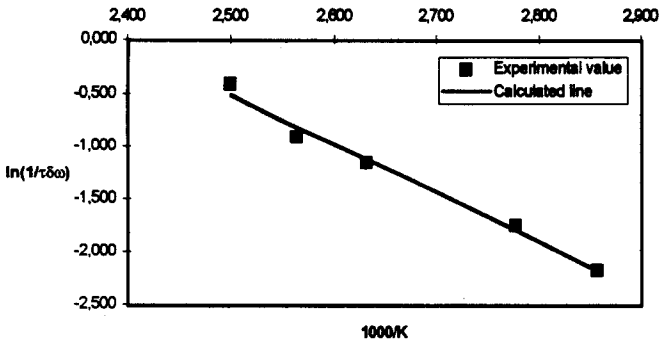

Figure 4. Temperature dependence of the reorientation rate constant ($1/2\tau$) for compound **1**. The energy barrier to reorientation obtained from this plot is 9.25 kcal/mol.

of the trajectories gives a picture of the rapid molecular motions characteristic of these compounds and helps in the interpretation of the results concerning the ^{13}C NMR relaxation rates. The dynamic characteristics are determined by the rotation of the piperazine moiety in position 2 (dihedral angle α) and of the phenyl substituent in position 4 (dihedral angle β) with respect to the quinoline nucleus (Chart 1). In the crystal structure of compound **1**, the piperazine moiety is constrained to be nearly coplanar with the quinoline nucleus, the α angle being about 14°. This packing requirement is promptly released by minimization and, during the simulation period of the dynamic run the piperazine substituent rapidly samples a range of conformations comprised between a dihedral angle of −40° and −100° with respect to the quinoline nucleus. A very similar behaviour of this moiety is observed for all the compounds studied (**1**, **2** and **4**) both in their neutral and protonated forms. The dynamic features of the phenyl substituent with respect to the quinoline nucleus are described in Figure 5, where the histograms cluster all the conformers sampled on the basis of the value of their torsional angle during the simulation. Ninety-six percent of the conformers sampled for compound **1** show a dihedral β angle comprised between −45° and −60° with an average value of −52.8°, the same as that found in the crystal structure. In the case of compound **2**, 85% of the conformers sampled show β values comprised between −20° and −35°, with an average value of −26.3°. On the contrary, the phenyl substituent of compound **4** samples a wider conformational space in the simulation time and significant conformer populations are found in the range of the torsional angles between −60° and −120°, the average value being −90.9°. It is interesting to note that, although the conformational space sampled by compounds **1** and **4** overlaps in the zone of the low angles, the conformer population of compound **4** in the range of β values comprised between −45° and −60° is less than 8%. The superimposition of the minimized average structure of compounds **1**, **2** and **4** is reported in Figure 6. A very similar picture is obtained from the simulations of the protonated forms of these compounds.

Table 6. Parameters of Gutowsky–Holm analysis of compound **1**

T_2 (s)	$\delta\omega_\infty$ (Hz)	T_c (K)	E_a (kcal/mol)	ν_0 (s^{-1})
0.96	97.8	410	9.25	3.36×10^6

Electronic property analysis. The electronic properties of the optimized structures were analysed and compared with one another with the twofold goal of investigating on the mutual influence of the electronic structure distribution on the conformation assumed, and on the role of these properties in the functional behaviour of the ligands with respect to the 5-HT$_3$ receptor.

The most informative indices, computed on the AM1 optimized structures of the compounds **1–4** in their neutral and protonated forms, are reported in Table 7

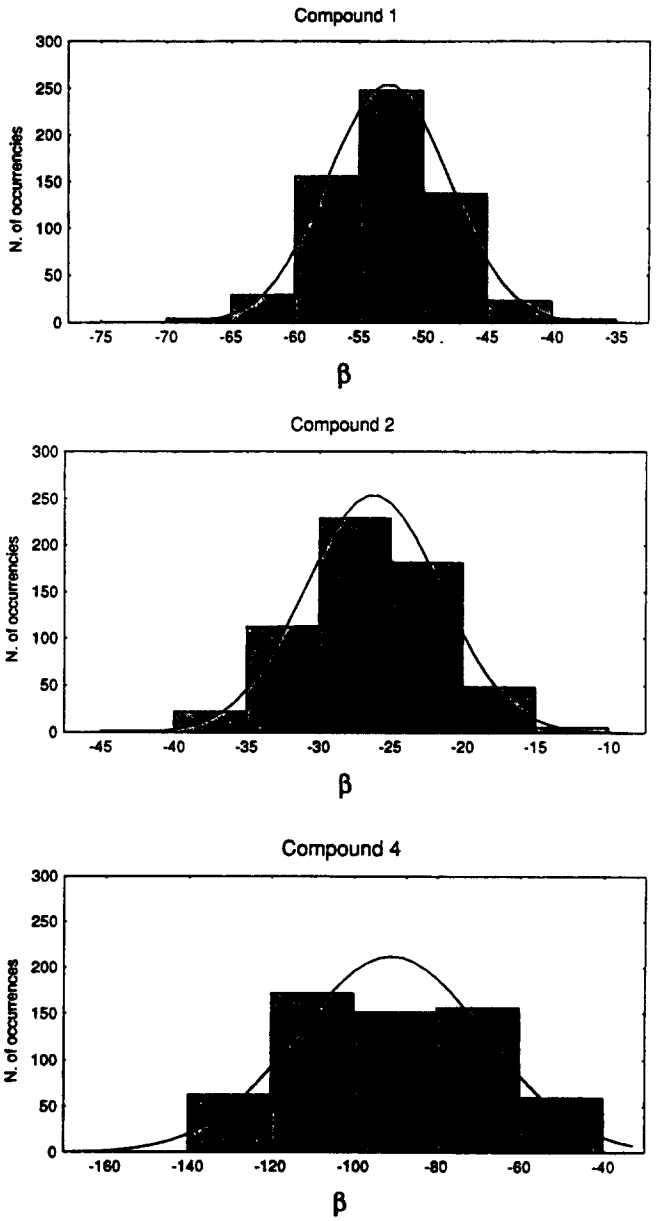

Figure 5. Torsional angle (β) distribution function for compounds **1**, **2** and **4** in their neutral forms.

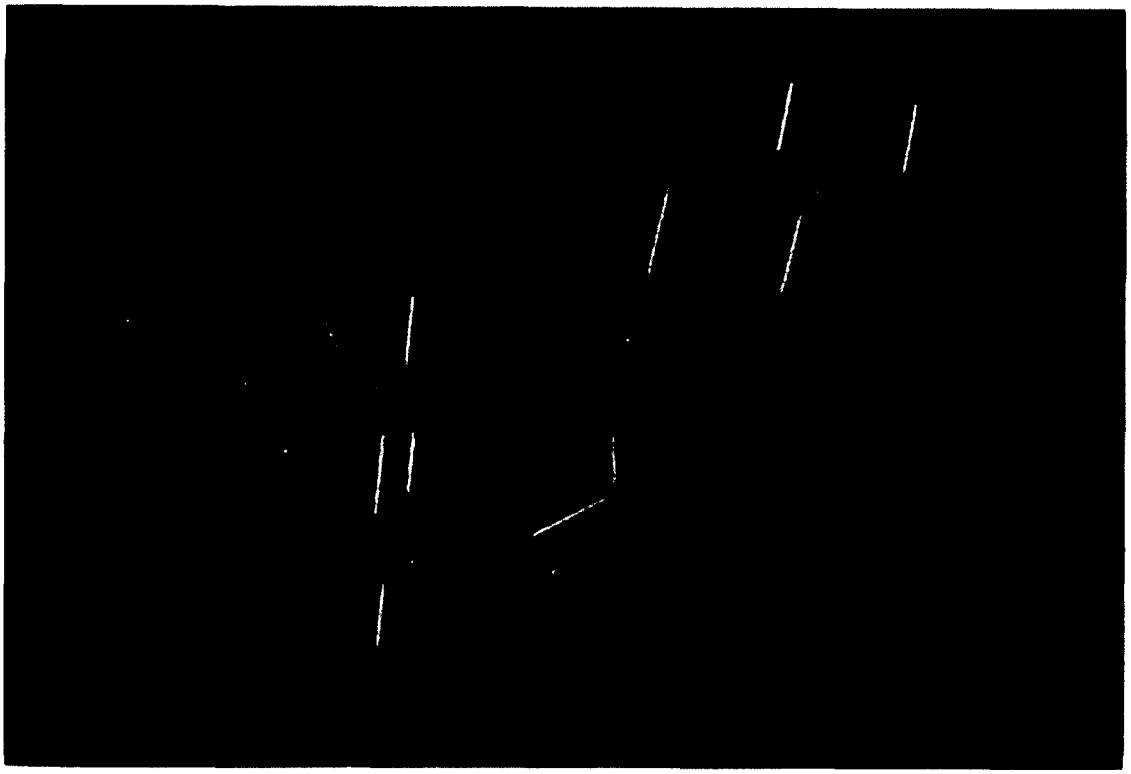

Figure 6. Superimposition of the minimized average structure of compounds **1** (green), **2** (violet) and **4** (blue).

together with the electronic features of the agonist quipazine and the antagonists ondansetron and LY278584. They are: S(L)D—nucleophilic superdelocalizability on the protonated nitrogen atom (hydrogen bond donor propensity). S(H)A—electrophilic superdelocalizability on the hydrogen-bond acceptor atom (i.e., the quinoline nitrogen atom of compounds **1–4** and of quipazine, and the carboxylic oxygen atom of ondansetron and LY278584). ΣS(H)Φ —sum of the electrophilic superdelocalizability on the carbon atoms of the phenyl substituent in position 4 of compounds **1–4**, and of the indole and indazole moieties of ondansetron and LY278584, respectively. ΣS(H)CS—sum of the electrophilic superdelocalizability on the heavy atoms of the entire condensed heterocyclic system. The last three indices are reported for the protonated and neutral forms of the compounds studied. The affinity of these ligands for the 5-HT_3 receptor is also listed.

Lipophilicity calculations and measurements

Log *D* calculation. Lipophilicity values were calculated using the PALLAS software (version 1.2, Compudrug Ltd, 1995), which is based on Rekker's collection of hydrophobic fragmental constant[17] derived from an extended 'knowledge engineering' improved set of about 1000 log *P* values in the 1-octanol/water system together with a pK_a correction giving log *D* profiles (Fig. 7).

Log *D* determination by pH-metric titration. The approach used for lipophilicity determination in this case represents an extension of the potentiometric

Table 7. Reactivity indices computed on compounds **1–4**, ondansetron, LY278583 and quipazine

	K_i[a] (nM)	Protonated form				Neutral form		
		S(L)D 10^2	S(H)A 10^3	ΣS(H)Φ 10^3	ΣS(H)CS 10^3	S(H)A 10^3	ΣS(H)Φ 10^3	ΣS(H)CS 10^3
Agonist								
Quipazine	1.2	0.5954	0.6046		7.520	1.024		6.670
Antagonists								
1	3.8	0.5768	0.6230	2.1606	7.772	1.0140	1.5647	9.643
2	1.6	0.6093	0.5156	3.6893	7.787	0.8981	3.2912	9.599
3	3.5	0.5861	0.6057	3.1288	7.808	0.9626	2.7948	8.566
4	34	0.5832	0.6302	2.2220	7.780	1.1290	0.2087	6.988
Ondansetron	1.2	0.3505	0.2929	4.3539	7.056	0.3973	4.6790	9.254
LY278584	0.7	0.5994	0.0770	4.9046	7.698	0.0613	5.5580	9.334

[a]For quipazine, ondansetron, and compounds **1–4** see ref (6); for LY278584 see ref (7).

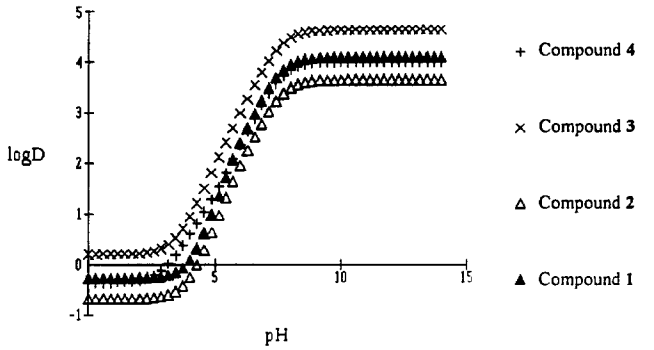

Figure 7. Log *D* profiles as calculated using the Pallas software.

procedure[18] and was developed by Avdeef et al.[19] Assays were done on the SIRIUS PCA101.[20] To measure lipophilicity by this technique pK_a values must be known a priori. Therefore, we first titrated solutions of our compounds in background electrolyte solution with standardized acid and base and estimated pK_a values from the difference curve which was obtained from the sample titration minus the blank titration curve. After adding 1-octanol a second titration was done. Since pK_a values (now referred to as p$_o K_a$) are shifted in the presence of the partitioning solvent, knowing the 1-octanol/water ratio, the effective partition at any pH can be readily determined from the calculated log *D* distribution curve (eq 4).

$$\log P = \log[10^{\Delta pK_a} - 1] - \log[V_{org}/V_{water}], \quad (4)$$

where $\Delta pK_a = pK_a - p_o K_a$

Titrations were run at 25 °C under an argon atmosphere to minimize absorption of atmospheric CO_2. Typically, 10 mg of the compound were dissolved into 10.0 mL of a background electrolyte solution (0.15 M KCl) and 0.5 mL of 0.5 M KOH was added. For the pK_a determination this solution was titrated with 0.5 M HCl from pH 12 to 2. After addition of 1.0 mL of 1-octanol the mixture was titrated back to pH 12 using 0.5 M KOH.

Log *D* curves (Fig. 8) were calculated employing the PKALOGP 3.2 evaluation software[20] from the shift of the pK_a values measured in water solution and the $p_o K_a$ values measured in a mixed water–organic solvent solution. The log *D* values obtained (at pH 7.4) in this way are given in Table 8.

Chemistry

The single crystal diffraction studies performed on compound **1** showed an asymmetric unity comprised of of three different molecules;[6] two of these showed negligible differences while the third represented the atropoisomeric form of the two others. Figure 9 shows the superimposition of the three molecules from the asymmetric unit found for compound **1**.

Because of the high affinity, activity and selectivity of 5-HT$_3$ receptor antagonist **1**, it appeared of interest to investigate on the possiblity of resolving **1** into the two atropoisomeric forms. Several approaches were tried to reach this goal.

In the first instance, we derivatized the oxepinoquinoline nucleus with a chiral amine by reaction of imidoyl chloride **5**[6] with (+)-(*R*)-α-phenylethylamine[21] to give compound **6** (Scheme 1).

The ^{1}H NMR spectrum of compound **6** in $CDCl_3$ showed a signal pattern attributable to a single compound, but when the ^{1}H NMR spectrum was performed using benzene-d_6 as solvent the split of the α-methyl signal into two doublets with approximately the same intensity (of 1.5 H) clearly indicated the presence of two diasteromeric forms of compound **6** in solution. The separation of the diasteromeric mixture of **6** was attempted by using the usual chromatographic techniques (preparative TLC and flash chromatography), but no detectable enrichment of the mixture in one of the two diasteromers was observed. These findings suggest the occurrence of the condensed heterocyclic system of **6** in two atropoisomeric forms separated by a potential energy barrier too low to allow the separation of the diasteromeric mixture of **6**.

This assumption appears to be also supported by the results of the ^{1}H NMR studies performed on compound **1** by using chiral solvating agents (CSA) such as (−)-(*R*)-1,1′-binaphthyl-2,2′-diylphosphoric acid (BNPPA).[22] The ^{1}H NMR spectrum of **1** in $CDCl_3$ in the presence of the stoichiometric amount of (−)-(*R*)-BNPPA showed a set of signals attributable to a single product, and also in this case using benzene-d_6 instead of $CDCl_3$ as solvent, a signal pattern attributable to a diasteromeric mixture appeared. The signal of the methyl group on the terminal piperazine nitrogen atom appeared to be split into two well separated singlets. Furthermore, other signals in the aromatic part of the spectrum were split by the use of BNPPA. Other CSA such as α-methoxy-α-(trifluromethyl)-phenylacetic acid (MTPA) appeared to be ineffective with compound **1** when either benzene-d_6 or $CDCl_3$ were used as solvents.

Interestingly, the use of benzene-d_6 as solvent was found to be essential to observe signal splitting both in the case of diasteromeric compound **6** and of the diasteromeric salt of **1** with BNPPA. This result could be explained by the great distance between the two chiral centres of the diasteroisomers: benzene seems to be able to transport the chiral information better than $CDCl_3$ probably by virtue of its π–π stacking and magnetic anisotropy properties.

Attempts to resolve compound **1** by recrystallization with BNPPA were unsuccessful.

The ^{1}H NMR spectroscopy studies performed at variable temperature indicated a racemization barrier $E_a = 9.25$ kcal/mol[15] ($\Delta G^* = 21.3$ kcal/mol) which accounts for the unsuccessful resolution of compound **1**. Unfortunately, because of the low racemization

barrier showed by compound **1**, it did not seem possible to investigate the binding stereospecificity of this compound.

Discussion

A deeper understanding of the structure–activity relationships of these ligands at molecular and sub-molecular level can be obtained by the comparative analysis of their geometry, molecular dynamics, electronic structure and lipophilicity.

In this respect, the comparison between compounds **1** and **4**, which differ only by an ethyleneoxy bridge, appears to be particularly interesting. The phenyl substituent of **4** is energetically [6]allowed to get a conformation superimposable on that of compound **1**, although the chance of finding the isolated molecule in this conformation at room temperature is very low. Interestingly, the NMR studies reported here showed good agreement between the structure of **1** in solution, the X-ray structure and the lowest energy conformer found by molecular mechanics.

With respect to its interaction with the receptor the ethyleneoxy moiety can be considered to perform two main functions: (a) to establish specific interactions mainly through its oxygen atom which in principle can behave as a hydrogen bond acceptor; (b) to contribute to the global lipophilicity of compound **1**. A comparison of the affinity data values of compounds **1–3** (Table 8) suggests that no strong interactions are established between this atom and the receptor; moreover, a graphic inspection of the superimposition of compounds **1** and **2** fails to reveal significant differences in the spatial positions of their phenolic oxygen atoms. Furthermore, the experimental determination of the lipophilicity (expressed as log *D* in Table 8)

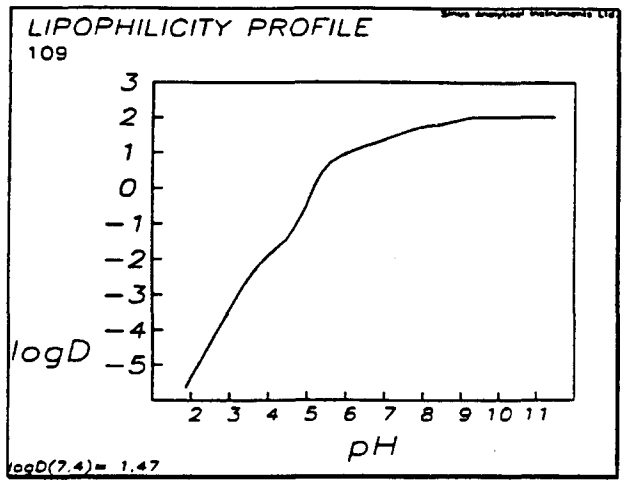

Compound 1

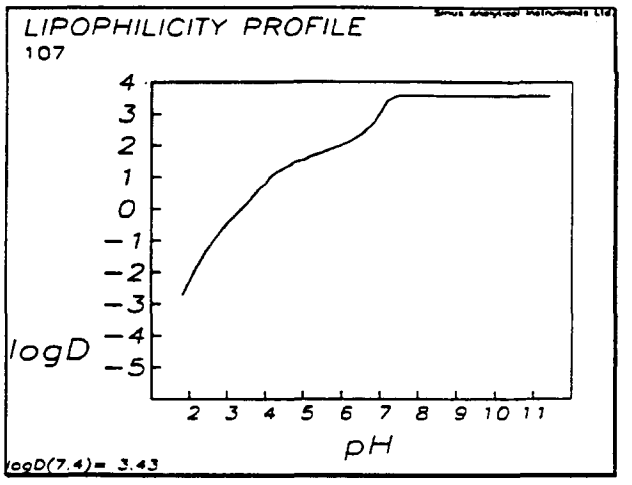

Compound 2

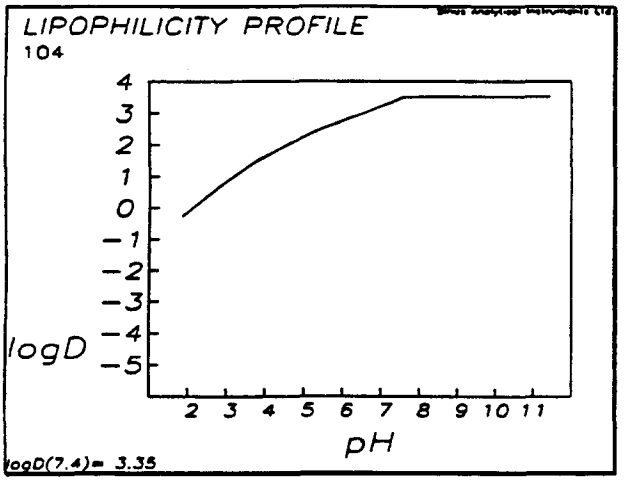

Compound 3

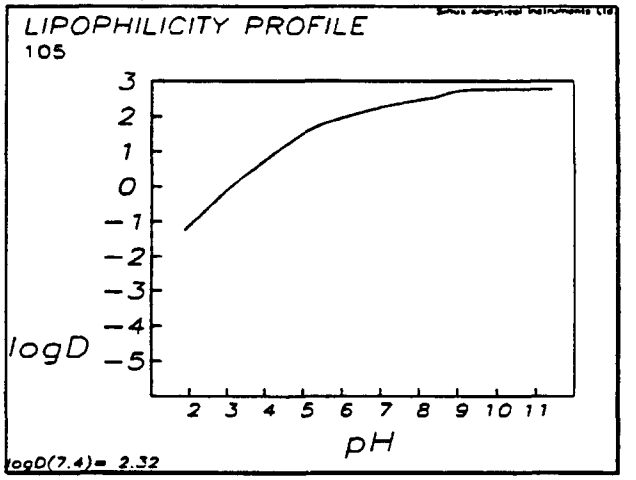

Compound 4

Figure 8. Lipophilicity profiles of compounds **1–4** measured by pH-metric titration.

Table 8. Selected physicochemical characteristics of compounds **1–4**

Compound	K_i (nM)[a]	ΔG[b]	β[c]	log D[d]	
				Calculated	Measured
1	3.8	−11.47	52.8°	3.67	1.47
2	1.6	−11.99	26.3°	3.21	3.43
3	3.5	−11.53	—	4.22	3.35
4	34	−10.18	90.9°	3.57	2.32

[a]See ref 6.
[b]The free energy of binding was calculated by the equation: $\Delta G = -RT \ln K_i$ (T=298 K).
[c]β is the average value of the dihedral angle between the phenyl substituent and the quinoline nucleus from the molecular dynamics simulations.
[d]log D values are reported as lipophilicity index and were calculated by using the PALLAS software or measured by pH-metric titration (as reported in the relative section); in both cases the log D values are referred at pH 7.4.

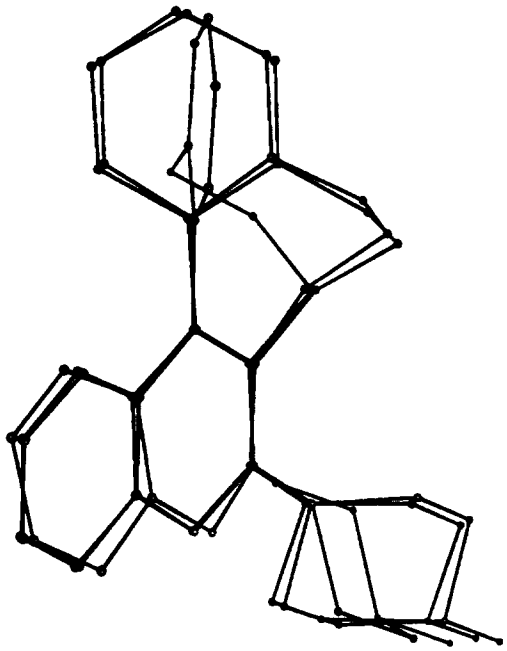

Figure 9. Superimposition of the three structures of compound **1** found in the asymmetric unity by X-ray diffraction studies.

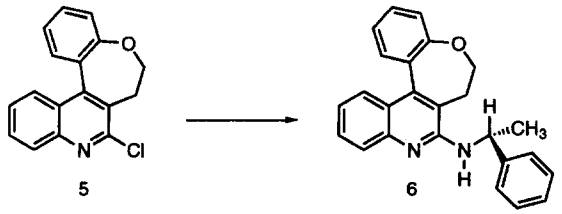

Reagents: (+)-(*R*)-α-Phenylethylamine

Scheme 1.

shows that compound **4** is significantly more lipophilic than compound **1** at pH 7.4 (see also Fig. 8). It is worth noting that, in this limited series of ligands, no correlation is observed between the lipophilicity and the 5-HT$_3$ receptor affinities; in fact, compound **1** is the least lipophilic but one of the most active.

From the experimental evidence collected in the studies reported here, we have developed the molecular dynamics picture of compound **1** discussed below.

At room temperature, piperazine slowly interconverts between the two chair forms and rapidly oscillates around its attachment bond at the heteroaromatic nucleus. The phenyl substituent is constrained by the ethyleneoxy bridge and rapidly vibrates within a very small angle around the position of the energy minimum (the dihedral angle between the phenyl substituent and the quinoline nucleus being about 50°) and slowly flips (low frequency flipping) from one atropoisomeric form to the other. The molecular dynamics model of compound **4** which emerges from these studies appears to be very similar to that found for compound **1** as far as the piperazine moiety is concerned, but the motions of the phenyl substituent in the 4-position of the quinoline nucleus appear to be very different. In fact, at room temperature, it rapidly oscillates sampling a conformational space almost perpendicular to the plane of the quinoline nucleus.

In conclusion, compounds **1** and **4** show very similar geometries and conformational preference and not very different lipophilicities, but the molecular dynamics of their condensed heterocyclic systems is rather different. On this basis a rationalization in terms of intermolecular interactions can be attempted by assuming that the phenyl substituent of **1** and **4** interacts by dispersive forces (charge transfer or π–π stacking) with a suitable amino acid residue in the receptor (e.g., a tryptophan residue).[23] In this case, the dynamic prerequisite for the interaction could be quite strict and compound **1** would show better prerequisites than **4**.

In this context, a detailed picture of the reactivity determinants of compounds **1–4** is reported in Table 7. The electronic features of the agonist quipazine and antagonists (R)-ondansetron and LY278584 are also reported in Table 7 in order to get an insight into the functional behaviour of these compounds towards the 5-HT$_3$ receptor. The molecular reactivity indices listed mimic the propensity of the ligands to give intermolecular interactions.[24] The selection of the descriptors, in the large amount available from the electronic wavefunction, was based on the three-dimensional pharmacophore models for the 5-HT$_3$ recognition site derived by computational techniques.[25] According to these models, the chemical template containing the recognition elements are an aromatic or heteroaromatic ring system, a coplanar carbonyl or equivalent group, and a basic nitrogen, interrelated by well-defined distances. [The critical assumption common to

these studies is that all compounds (agonists or antagonists) bind at the same receptor site].[25]

A qualitative analysis of the data values reported in Table 7 shows that, in such a small sample of compounds, variations in the 5-HT_3 binding affinity data values do not correspond to any significant and/or organized variation in the values of the hydrogen-bond donor/acceptor reactivity descriptors. Moreover, these indices do not discriminate between agonists and antagonists. In fact, the agonist quipazine shows S(L)donor and S(H)acceptor values in between those of the antagonists. On the contrary, the most striking observations arise from the analysis of the electronic indices on the aromatic rings and on the condensed heterocyclic systems. In the small series of congeneric compounds **1–4** studied, the variation in the binding affinity roughly parallels the variation in the $\Sigma S(H)\Phi$ for both the protonated and neutral forms. Owing to the preference of the phenyl substituent in position 4 for a β angle of 90°, compound **4** is characterized by the lowest values of the $\Sigma S(H)\Phi$ and $\Sigma S(H)CS$, while these indices show the highest values for compound **2**, in which the phenyl substituent is constrained in a quasi planar position.

Moreover, the protonated agonist and antagonists exhibit the same values of $\Sigma S(H)CS$, while this index discriminates between the two functional categories of ligands when the neutral forms are considered. This seems to suggest that dispersion interactions of the condensed heterocyclic systems might give an important contribution to both the recognition and binding steps, and/or that the recognition step is essentially determined by the long-range electrostatic interactions of the protonated nitrogen, while dispersion forces contribute to a different extent to the binding of the antagonists, once the main docking has been accomplished.

In other words, once the hydrogen-bond donor/acceptor requirements are satisfied, the functional activity and, perhaps, the binding affinity might be modulated by the optimization of short-range intermolecular interactions and dispersion contribution of the condensed heterocyclic system with suitable amino acids of the receptors.

On the basis of the analogies emerging from the comparative analysis of the electronic features of the isolated ligands, the superimposition of ondansentron, LY278584 and compound **2** shown in Figure 10 can be proposed. The dummy atoms used in the fitting (represented as dots in the figure) simulate two key residues of the receptor capable of giving electrostatic and dispersive interactions with the ligands. According to Swain et al.,[25] the basic nitrogen in both agonists and antagonists occupies a common binding site but the rest of the functionally divergent ligands fits different pockets in the receptor. The idea of different but overlapping sites for the 5-HT_3 agonists and antago-

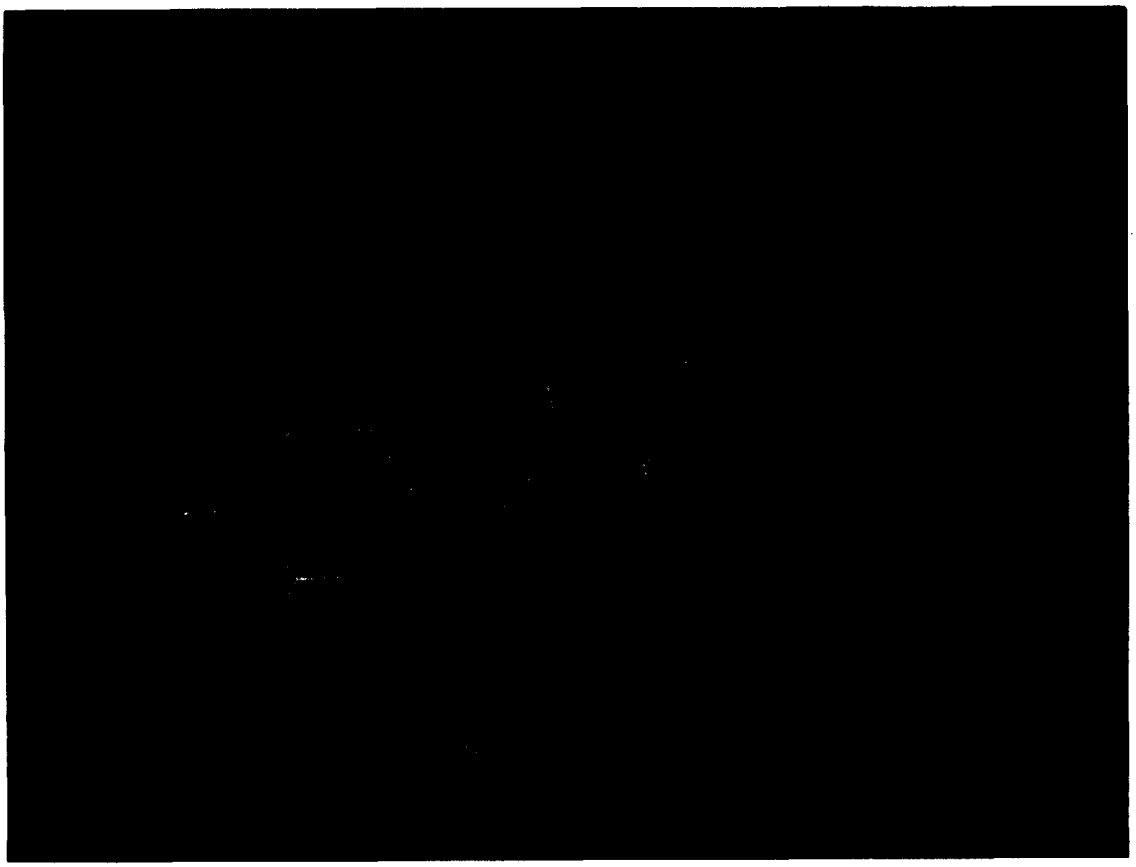

Figure 10. Mapping of the 5-HT_3 antagonist binding site by superimposition of compound **2** (green), ondansetron (violet) and LY278584 (blue)

nists seems to be supported by our model based on the reactivity indices. In fact, the close similarity of the $\Sigma S(H)\Phi$ indices of these antagonists suggests a common mode of interaction of the phenyl substituent of compounds **1–3** and the condensed benzo ring of ondansentron and LY278584, which occupy the antagonist binding site of the receptor. The quinoline moiety of compounds **1–3** occupies a zone of the 5-HT$_3$ receptor which might or might not coincide with the agonist binding site. However, in the first hypothesis, the unambiguous antagonist nature of compounds **1–3**[6] might be explained by the differences in the electronic distribution on the quinoline moiety of quipazine and ligands **1–4** (Table 7). In fact, the presence of the substituents significatively reduces the reactivity potential of the quinoline moieties of the antagonists ($\Sigma S(H)$ for the quinoline moiety ranges from the values of 4.1×10^{-3} to 5.6×10^{-3} for ligands **1–4**, while it is 7.5×10^{-3} for quipazine) and this might be responsible for the unproductive binding at the agonist site.

Conclusion

The importance of the dynamic characteristics of a limited series of 5-HT$_3$ antagonists in receptor binding and their role in affecting the receptor affinity has been emphasized in this work on the basis of experimental and theoretical studies. Moreover, a comparative analysis of the electronic features of the isolated ligands allowed us to identify two potential key interactions with the receptor (electrostatic and dispersive interactions) and to propose a model for the 5-HT$_3$ receptor binding capable of distinguishing between functionally divergent ligands by virtue of the reactivity determinants of their aromatic moieties.

Experimental

NMR

^{1}H NMR data were obtained on Bruker AC 200 and Bruker AMX 600 spectrometers operating at 200.13 and 600.14 MHz proton Larmor frequency, respectively. The temperature value was in the range of 298–410 K in the case of the variable temperature studies; it was 298 K in all other cases.

^{1}H non-selective and ^{13}C spin lattice relaxation rate were performed at 200 MHz using the $(180°-\tau-90°-t)n$ pulse sequence. The ^{13}C inversion-recovery was performed using broad-band decoupling. The relaxation time values were obtained using a three parameter calculation.

Correlation times of the ^{1}H–^{13}C vectors were calculated using eq (1).[11]

2D experiments (MCOSY,[26] NOESY, 2D *J*-resolved[27] and HETCOR) were performed on the 600 MHz spectrometers. NOESY data were collected using the TPPI method.[28] Arrays of 512 FID, of 1024 data points, were acquired. The sine-bell squared weighing function with 45°–60° phase shift was applied to the data. The HETCOR experiment was performed by $[(\pi/2)_H-t_{1/2}-\pi_C-t_{1/2}-(\pi/2)_H(\pi/2)_C-AT]$ pulse sequence.[29]

Computational methods

The input structure of compounds **1** and **2** was obtained from their X-ray coordinates.[6] The starting geometries of the other derivatives considered (**3** and **4**) were constructed within the Chemnote module of the program Quanta 4.1.[30] The structure of the agonist quipazine and the antagonists ondansetron (R enantiomer) and LY278584 were also studied for comparative purposes. Complete geometry optimizations were performed by means of molecular orbital AM1 calculations[31] using the MOPAC program (QCPE 455). Both the neutral and protonated forms of the compounds considered were studied.

Molecular dynamics simulations were performed on compounds **1**, **2** and **4**. The structures were minimized using the CHARMm[32] package until the root-mean-square (rms) potential energy gradient was less than 0.1 kcal mol^{-1} Å^{-1}. Then they were thermalized to 300 K with a 5 K rise per 100 steps by randomly assigning individual velocities from a Gaussian distribution. After heating, the systems were allowed to equilibrate for 44 ps and the velocities were scaled by a single factor. An additional 20 ps period of equilibration with no external perturbation was allowed. Conformations were recorded every 0.5 ps of a 300 ps trajectory and the time-average structure was calculated and minimized.

A distance dependent dielectric constant ($\varepsilon=4r$) was employed in order to reduce the long-range electrostatic term and to incorporate some effects of the solvent.

Superposition of compound **2**, ondansetron and LY278584 was obtained by a rigid fit procedure, minimizing the rms deviations of three dummy atom pairs defined as follow: (a) a dummy atom positioned at 3 Å from the protonated nitrogen on the vector defined by the N—H bond, (b) two dummy atoms positioned at 2 Å above and below the centre of the aromatic ring farthest from the the protonated nitrogen group.

Calculations were performed on a HP720 workstation.

Chemistry

Melting points were determined in open capillaries on a Gallenkamp apparatus and are uncorrected. Microanalyses were carried out using a Perkin–Elmer 240C Elemental Analyser. Merck silica gel 60, 70–230 mesh, was used for column chromatography and Merck DC-Fertigplatten Kieselgel 60 F_{254} were used for TLC. ^{1}H NMR spectra were recorded with a Bruker AC 200 spectrometer in the indicated solvents (TMS as internal standard): the values of the chemical shifts are

expressed in ppm and coupling constants (J) in Hz. NMR spectra and elemental analyses were performed in the Dipartimento Farmaco Chimico Tecnologico, Università di Siena. The optical rotation was determined with an Optical Activity polarimeter type AA-5.

(*R*)-6,7-Dihydro-8-(1-phenylethylamino)-[1]benzoxepino[4,5-*c*]quinoline (6). A mixture of the iminochloride **5**[6] (0.1 g, 0.35 mmol) in (+)-(*R*)-α-phenylethylamine (3.0 ml, 23.3 mmol) was heated to reflux under argon for 22 h, then the reaction mixture was concd under red. pres. and the residue was purified by column chromatography. Elution with *n*-hexane:ethyl acetate (8:2) yielded pure **6** (0.11 g, yield 86%). Mp 150–153 °C; $[\alpha]_D^{21}$ +162.5 (*c* 0.4; $CHCl_3$). ^1H NMR ($CDCl_3$): δ 1.67 (d, J=7.0 Hz, 3H), 2.49–2.59 (m, 1H), 2.68–2.88 (m, 1H), 4.43–4.57 (m, 2H), 4.83 (d, J=6.7 Hz, 1H), 5.59–5.73 (m, 1H), 7.06–7.68 (m, 11H), 7.73–7.78 (m, 2H); (benzene-d_6) 1.53 (d, J=6.9 Hz, 1.5H), 1.62 (d, J=6.9 Hz, 1.5H), 1.65–1.77 (m, 1H), 2.21–2.45 (m, 1H), 3.96–4.19 (m, 2H), 4.50 (d, J=6.2 Hz, 1H), 5.83–5.97 (m, 1H) 6.95–7.24 (m, 7H), 7.34–7.45 (m, 4H), 7.84 (d, J=8.4 Hz, 1H), 8.11 (d, J=8.1 Hz, 1H). Anal calcd for $C_{25}H_{22}N_2O$: C, 81.94; H, 6.05; N, 7.64. Found: C, 82.30; H, 6.10; N, 7.32.

Acknowledgements

The authors wish to thank Prof. Michel Hamon (Neurobiologie Cellulaire et Fonctionnelle, INSERM U. 288, Faculté de Medicine Pitié-Salpêtrière, Paris) and Prof. Claudio Rossi (Dipartimento di Chimica, Università di Siena) for their collaboration. Thanks are due to the Italian MURST (40 and 60% funds) for financial support.

References and Notes

1. (a) Roca, J.; Artaiz, I.; Del Rio, J. *Exp. Opin. Invest. Drugs* **1995**, *4*, 333. (b) Bentley, K. R.; Barnes, N. M. *CNS Drugs* **1995**, *3*, 363.

2. (a) Ireland, S. J.; Tyers, M. B. *Br. J. Pharmacol.* **1987**, *90*, 229. (b) Round, A.; Wallis, D. I. *Neuropharmacology* **1987**, *26*, 39.

3. Barnes, J. M.; Barnes, N. M.; Costall, B.; Jagger, S. M.; Naylor, R. J.; Robertson, D. W.; Roe, S. Y. *Br. J. Pharmacol.* **1992**, *105*, 500.

4. Emerit, M. B.; Riad, M.; Fattaccini, C. M.; Hamon, M. *J. Neurochem.* **1993**, *60*, 2059.

5. Bolanos, F. J.; Schechter, L. E.; Miquel, M. C.; Emerit, M. B.; Rumigny, J. F.; Hamon, M.; Gozlan, H. *Biochem. Pharmacol.* **1990**, *40*, 1541.

6. Anzini, M.; Cappelli, A.; Vomero, S.; Giorgi, G.; Langer, T.; Hamon, M.; Merahi, N.; Emerit, B. M.; Cagnotto, A.; Skorupska, M.; Mennini, T.; Pinto, J. C. *J. Med. Chem.* **1995**, *38*, 2692, and references cited therein.

7. Wong, D. T.; Robertson, D. W.; Reid, L. R. *Eur. J. Pharmacol.* **1989**, *166*, 107.

8. Hino, K.; Kawashima, K.; Oka, M.; Uno, H.; Matsumoto, J. *Chem. Pharm. Bull.* **1989**, *37*, 190.

9. Macromodel 3.0 Columbia University, New York, 1991.

10. In this paper we follow the convention that the molecular motions which satisfy the relationship $\omega_0\tau_c << 1$ have to be considered rapid. Thus, the molecular motions characterized by τ_c values in the order of ps are referred to as rapid motions.

11. Allerhand, A.; Komoroski, R. A. *J. Am. Chem. Soc.* **1973**, *95*, 8228.

12. Gutowsky, H. S.; Holm, C. H. *J. Chem. Phys.* **1956**, *25*, 1228.

13. Gutowsky and Holm claimed that if the line widths ($1/T_2$) are small compared to the separation δω the observed separation is not influenced by the overlap of the components and depends only on τ. Only when $1/T_2\delta\omega > 1/3$, the overlap of the components became significant. In the GH-method it is suggested that the T_2 value should be found by measuring the line-width under such conditions of coalescence that the resonance components had coalesced to a single line ($\tau \rightarrow 0$). The $\delta\omega_\lambda$ value (97.8 Hz) was determined also from measurements performed at 600 MHz and it was found to be stable in the temperature range of 298–338 K. Taking the T_2 value (0.96 s) together with the $\delta\omega_\lambda$ value, in our case, the $1/T_2\delta\omega$ value is lower than 1/3 and the overlap effect can be neglected. Unfortunately, our case is complicated by the fact that the line shapes are also affected by the strong coupling in the ABMX system. Thus, some degrees of uncertainty can derive from the approximation in $\delta\omega_c$ measurement, and also an E_a value of about 15 kcal/mol is compatible with the experimental results. However, even if a more rigorous approach by means of computer line shape simulations can give more precise results, we consider the present results to be sufficiently significant for our purposes.

14. Eyring, H. *Chem. Rev.* **1935**, *17*, 65.

15. The E_a value found for the interconversion of the condensed heterocyclic system of **1** appears to be well correlated with the value previously reported for compound **7**.

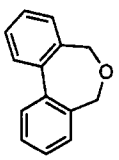

7

Kurland, R. J.; Rubin, M. B.; Wise, W. B. *J. Chem. Phys.* **1964**, *40*, 2426. For related work on bridged biphenyls see also Mislow, K.; Glass, M. A. W.; Hopps, H. B.; Simon, E.; Wahl, G. H. *J. Am. Chem. Soc.* **1964**, *86*, 1710, and references cited therein.

16. The $t_{1/2}$ value for the interaction of **1** with 5-HT_3 receptors was calculated as follows:

$t_{1/2} = 0.693/(K_d \cdot K_1)$ assuming $K_1 = 10^6$ M^{-1} s^{-1} (according to Bennett, J. P.; Yamamura, H. I. *Neurotransmitter Receptor Binding*; Yamamura, H. I.; Enna, S. J.; Kuhar, M. J., Eds; Raven Press: New York, 1985; pp 61–89) and $K_d = K_i$.

17. Rekker, R. F. *The Hydrophobic Fragmental Constant. Its Derivation and Application. A Means of Characterizing Membrane Systems*; Elsevier; Amsterdam, 1977.

18. (a) Seiler, P. *Eur. J. Med. Chem.—Chim. Therap.* **1974**, *9*, 663. (b) Kaufman, J. J.; Semo, N. M.; Koski, W. S. *J. Med. Chem.* **1975**, *18*, 647. (c) Clarke, F. H. *J. Pharm. Sci.* **1984**, *73*,

226. (d) Clarke, F. H.; Cahoon, N. M. *J. Pharm. Sci.* **1987,** *76*, 611.

19. (a) Avdeef, A. *QSAR: Rational Approaches to the Design of Bioactive Compounds*; Silipo, C.; Vittoria, A. Eds; Elsevier: Amsterdam, 1991, pp 119–122. (b) Avdeef, A. *Quant. Struct.–Activ. Relat.* **1992**, *11*, 510. (c) Avdeef, A. *J. Pharm. Sci.* **1993**, *82*, 183. (d) Avdeef, A.; Comer, J. E. A.; Thomson, S. J. *Anal. Chem.* **1993**, *65*, 42.

20. Sirius Analytical Instruments Ltd, Forest Row, England.

21. Feringa, B.; Wymberg, H. *J. Org. Chem.* **1981**, *46*, 2547, and references cited therein.

22. (a) Shapiro, M. J.; Archinal, A. E.; Jarema, M. A. *J. Org. Chem.* **1989**, *54*, 5826. (b) Parker, D. *Chem. Rev.* **1991**, *91*, 1441. (c) Arnold, W.; Daly, J. J.; Imhof, R.; Kyburz, E. *Tetrahedron Lett.* **1983**, *24*, 343. (d) Hibert, M. F.; Gittos, M. W.; Middlemiss, D. N.; Mir, A. K.; Fozard, J. R. *J. Med. Chem.* **1988**, *31*, 1087.

23. Miquel, M. C.; Emerit, M. B.; Gozlan, H.; Hamon, M. *Biochem. Pharmacol.* **1991**, *42*, 1453.

24. Cocchi, M.; Menziani, M. C.; De Benedetti, P. G.; Cruciani, G. *Chemometrics Intell. Lab. Syst.*, **1992**, *14*, 209.

25. (a) Schmidt, A. W.; Peroutka, S. J. *Mol. Pharmacol.* **1989**, *36*, 505. (b) Hibert, M. F.; Hoffmann, R.; Miller, R. C.; Carr, A. A. *J. Med. Chem.* **1990**, *33*, 1594. (c) Rizzi, J. P.; Nagel, A. A.; Rosen, T.; McLean, S.; Seeger, T. *J. Med. Chem.* **1990**, *33*, 2721. (d) Evans, S. M.; Galdes, A.; Gall, M. *Pharm. Biochem. Behav.* **1991**, *40*, 1033. (e) Swain, C. J.; Baker, R.; Kneen, C.; Herbert, R.; Moseley, J.; Saunders, J.; Seward, E. M.; Stevenson, G. I.; Beer, M.; Stanton, J.; Watling, K.; Ball, R. G. *J. Med. Chem.* **1992**, *35*, 1019. (f) Gozlan, H.; Langlois, M. *Central and Peripheral 5-HT$_3$ Receptors*; Hamon, M., Ed.; Academic: London, 1992, pp 59–83. (g) Gouldson, P. R.; Winn, P. J.; Reynolds, C. A. *J. Med. Chem.* **1995**, *38*, 4080.

26. Ane, W. P.; Bartholdi, E.; Ernst, R. R. *J. Chem. Phys.* **1975**, *64*, 2229.

27. Bodenhausen, G.; Freeman, R.; Morris, G.; *J. Magn. Reson.* **1976**, *23*, 171.

28. Marion, D.; Wuthrich, K. *Biochem. Biophys. Res. Commun.* **1982**, *113*, 967.

29. Bax, A. D.; Morris, G. A. *J. Magn. Reson.* **1981**, *42*, 50.

30. QUANTA/CHARMm, 1990 Polygen Corporation, 200 Fifth Avenue, Waltham, MA 02254 U.S.A.

31. Dewar, M. J. S.; Zoebisch, E. G.; Healey, E. F.; Stewart, J. J. P. *J. Am. Chem. Soc.* **1985**, *107*, 3902.

32. Brooks, B. R.; Bruccoleri, R. E.; Olafson, B. D.; States, D. J.; Swaminathan, S.; Martin, K. *J. Comput. Chem.* **1983**, *4*, 187.

(*Received in U.S.A.* 23 *February* 1996; *accepted* 1 *April* 1996)